

Design of the next-generation ultrahigh energy neutrino observatory PUEO

Q. Abarr^{a,*} for the PUEO Collaboration

^aDept. of Physics & Astronomy, University of Delaware

E-mail: qabarr@udel.edu

PUEO (the Payload for Ultrahigh Energy Observations) is a balloon-borne payload designed to detect the impulsive radio signals produced through the Askaryan effect by ultrahigh-energy (UHE) neutrinos (>1 EeV) in the Antarctic ice. Several key upgrades over its predecessor ANITA allow for an order of magnitude improvement in sensitivity to UHE neutrinos. These include an interferometric phased array trigger, newly designed antennas that double the overall collecting area above 300 MHz, a dedicated low-frequency instrument optimized for detection of air showers, and a roughly order-of-magnitude improvement in pointing resolution enabled by new inertial navigation systems. Through the combination of these improvements, PUEO is expected to have world-leading sensitivity to UHE neutrinos when it flies on a long duration balloon during the 2025-2026 austral summer from McMurdo Station, Antarctica.

38th International Cosmic Ray Conference (ICRC2023)
26 July - 3 August, 2023
Nagoya, Japan



*Speaker

1. Introduction

Ultrahigh-energy (UHE) neutrinos, though they have yet to be detected, will allow for unique study of astrophysical sources at the highest energy scales. Whether produced directly at the source [1, 2, e.g.] or through the interaction of UHE cosmic rays with the cosmic microwave background via the Greisen-Zatsepin-Kuzmin (GZK) effect [3, 4], UHE neutrinos would point back to their sources since they are not deflected by galactic magnetic fields as cosmic rays are.

PUEO (the Payload for Ultrahigh-Energy Observations) is a balloon-borne neutrino detector that builds on the success of ANITA (the Antarctic Impulse Transient Antenna), which set limits on UHE neutrino fluxes above 30 EeV over the course of four Antarctic flights between 2006 and 2016 [5–8]. ANITA, and now PUEO, are built upon the principle of detecting the impulsive radio signals produced by UHE neutrinos as they interact in the ice sheet of Antarctica, through a process called the Askaryan effect [9, 10]. We are able to improve the sensitivity by an order of magnitude over ANITA's by applying lessons learned during previous campaigns, as well as by using technologies which are novel to ballooning, such as a phased array trigger.

For more information on PUEO, see Reference [11]. A detailed look at the Askaryan detection channel can be found in Contribution [12].

2. The PUEO Instrument

The PUEO main instrument has a bandwidth of 300 MHz to 1200 MHz, with 108 antennas sensitive to both vertical and horizontal polarization; this gives a total of 216 channels in the main instrument. Additionally, a low-frequency drop-down instrument has a bandwidth of 50 MHz to 300 MHz. These are supported by a gondola structure made of aluminum and carbon fiber, designed for modular assembly which makes recovery in a remote location in Antarctica easier.

2.1 Dual-polarized quad-ridged horn antennas and signal chain

The main instrument bandwidth of 300 MHz to 1200 MHz increases the low-end cutoff from ANITA's 180 MHz. ANITA-III and ANITA-IV saw significant anthropogenic continuous wave (CW) signal below 300 MHz, rendering much of that band unusable. By increasing the cutoff, PUEO is able to shrink the antenna size by a factor of ~ 2 , thus more than doubling the collecting area at 300 MHz. The antennas are designed and produced by Toyon to have an individual effective gain of > 8.5 dB; by beamforming over the entire instrument, we expect to achieve an overall effective gain of > 20 dB.

Each antenna is sensitive to both vertically and horizontally polarized signals, and can separate them at the 5° level. This is essential for separating out background because neutrino Askaryan signals are primarily vertically polarized.

The antennas are arranged into five rings; the top four each consist of 24 antennas spanning 360° and canted downward 10° below horizontal since Askaryan events tend to come from just below the horizon, which is at 6° . The top ring consists of two rows of antennas due to launch envelope requirements, but these antennas have the same azimuthal spacing as the middle three rings. The bottom ring, called the 'nadirs', contains only twelve antennas spanning 360° and will

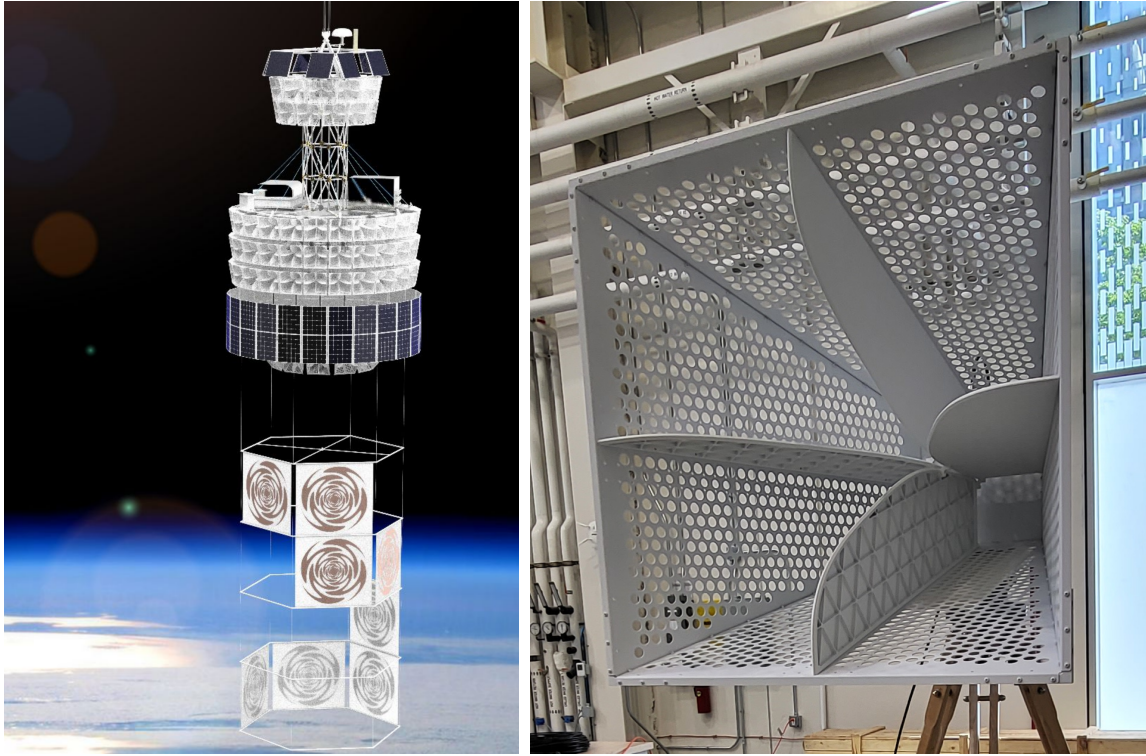


Figure 1: Left: Rendering of the PUEO payload in flight, with the Low Frequency instrument hanging beneath. Right: Close-up of a Toyon antenna

be canted downward at 40° . This increases PUEO's sensitivity to events produced by extensive air showers (EAS), which when tend to come from steeper angles when they reflect off the ice.

The top four rings of antennas are organized into 24 phi sectors, groups of vertically aligned antennas that cover 15° in azimuth. After deployment of the nadirs, the baseline height will be ~ 8.5 m; this gives a pointing resolution from interferometry of $< 0.15^\circ$ in elevation.

The signal from each antenna is fed directly into an antenna-mounted pre-amplifier (AMPA), which contains a Bree CNX filter, a low noise amplifier from SaP, and a bias tee. Each AMPA is connected by LMR195 cable to an RF receiver, which collects one polarization channel from eight antennas. The receiver design consists of two 20 dB amplifiers, a gain slope corrector, and another filter. This signal chain gives a gain response of $\sim (70 \pm 1)$ dB over the entire PUEO band.

2.2 Low Frequency Instrument

An important secondary science driver for PUEO is the detection and characterization of UHE cosmic rays through geometric radio emission produced by EAS in the upper atmosphere. To maximize this capability in PUEO, as well as increase the sensitivity of the tau neutrino detection channel, PUEO includes a dedicated drop-down instrument optimized for EAS signals; it can be seen suspended below the main payload in Figure 1.

The LF instrument has a band of 50 MHz to 300 MHz and eight dual-polarized sinuous antennas. Due to restrictions on the payload envelope during launch, the instrument is stored in the central column of PUEO and deploys after the payload reaches float. To meet these requirements, the LF

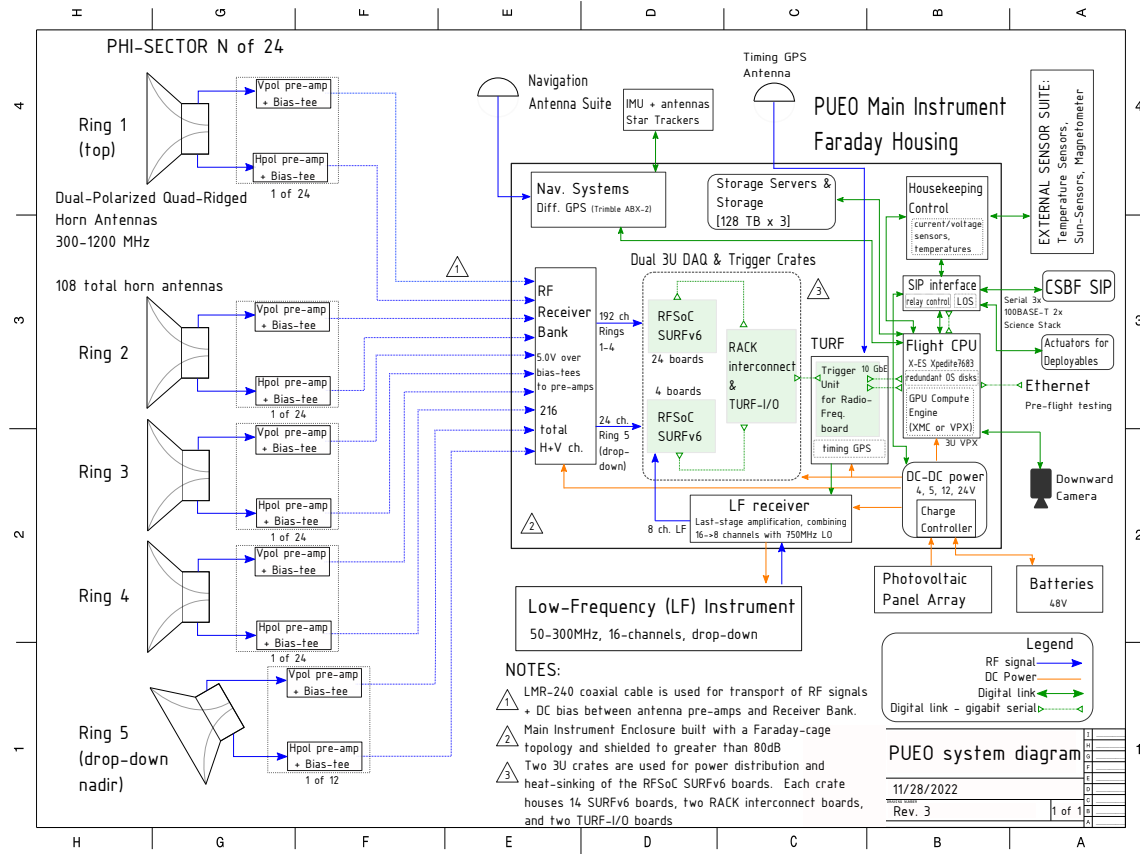


Figure 2: The system diagram of the entire PUEO payload

instrument will be constructed of horizontal hexagons of 1 inch carbon fiber tubes connected by Dyneema rope. The antennas themselves are made of conductive Ni/CuAg coating on ripstop nylon fabric sewn into polyester panels. Fully deployed, the LF instrument is 7 m tall, and is suspended 4.7 m below the main instrument. For a more detailed description of the low frequency instrument and the air shower detection channel of PUEO, see Contribution [13].

2.3 Data acquisition system

The DAQ contains twenty-eight sampling units (SURFs), four RACK interconnect boards, and four TURF-I/O boards which interface the SURFs with the trigger unit (TURF). These are divided equally between two 3U crates for power distribution and heat dissipation. Of the fourteen SURFs in each crate, twelve are for the main instrument. One crate contains two SURFs for the drop-down nadir antennas, while the other contains one for the nadirs and another for the LF instrument.

Each SURF is a custom board on which is mounted a Trenz TE0835 with a Xilinx ZU47DR RFSoc (Radio Frequency System-on Chip). This is a relatively new technology that enables much of PUEO's improvement, owing to its low power requirements that make it feasible to use as both trigger and digitizer on a balloon. The RFSoc combines fast, high-resolution analog-to-digital converters (ADCs) and digital-to-analog converters (DACs) in a single unit field-programmable gate array (FPGA). This differs significantly from ANITA, in which the triggering and digitizing

paths were physically separate due to power limitations.

2.3.1 Interferometric phased array trigger

The RFSocCs sample rate is 3 GHz, which allows PUEO to implement an interferometric phased array trigger. By taking the waveforms from adjacent antennas and coherently summing them with a range of time delays corresponding to different incident angles of the Askaryan plane wave, the uncorrelated thermal noise can be averaged down while retaining the strength of the signal, achieving an SNR increase proportional to \sqrt{N} , with N being the number of antennas. This has been successfully used in other radio neutrino experiments [14, e.g.].

The trigger is designed to reach a single-antenna threshold of 1σ over thermal noise. A simulation of this, using modified results from ANITA, is shown in Figure 3. At 50 % trigger efficiency this predicts a 0.8σ SNR for vertically polarized signals, a 5-fold improvement over ANITA-IV.

At the first of three trigger levels, L1, signals of the same polarization from pairs of adjacent phi sectors are digitized to 12-bits, and high- and low-pass filters are applied to maximize the SNR in the triggering band. The exact details of this are still under study based on simulations of the Toyon antenna characteristics, but the trigger bandwidth will be ~ 290 MHz to 700 MHz.

The waveforms are decimated to 4 or 5 bits (enough to preserve the results of triggering with 12 bits). The SURFs then beamform these 8 waveforms into ~ 50 beams, corresponding to signal arrival directions over 45° in elevation and 30° in azimuth. These directions are defined by a set of 'delay codes' for each antenna, which are applied by the firmware from a look-up table. This L1 processing is done at 100 Hz, and each snapshot is then sent to the SURF of its adjacent phi-sector over a 20 Gbit s^{-1} connection.

In the L2 trigger, beamforming is done on the L1 beams from adjacent phi sector pairs, now covering a total of four phi sectors and sixteen channels, equalling 60° in and 45° in elevation. Each phi sector is included in two L2 beams, on its own SURF and on its neighboring SURF, ensuring no azimuthal gaps in the trigger. The L2 beamforming is done at 5 Hz and results in ~ 100 new beams.

Finally, at the L3 trigger, each beam is checked to see if the power is above threshold, in which case it is sent over a 750 Mbit s^{-1} connection through one of the four TURF-I/Os, which are custom FPGAs, to the TURF to be written to disk. The TURF then forwards the data over redundant 10 Gbit Ethernet links to the flight computer.

2.4 Flight computer and data handling

The onboard computer will be an XE-S Xpedit 7638 with a 12-core Xeon D-1559 and 32 GB of RAM, running Alma Linux 8. The flight computer has two pathways for events it receives from

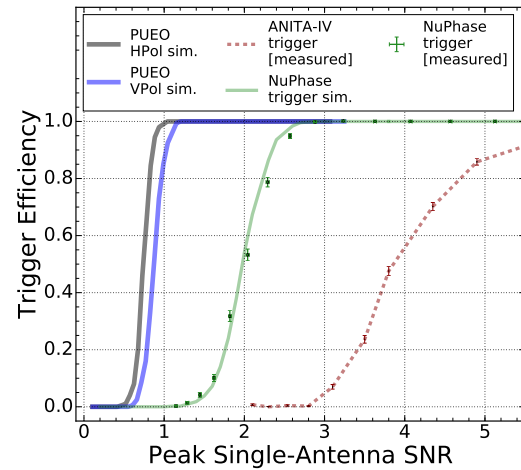


Figure 3: Simulated result for the PUEO beam-forming trigger, compared to measurements of ANITA's non-beamforming trigger and the phased array trigger from the Askaryan Radio Array [14].

the TURF. First, all events will be stored locally on the payload. Each PUEO event will be ~500 kB, which with an expected 100 Hz event rate and a 30 d flight, produces about 50 TB of data after compression. To prevent any loss of data, events will be stored in a triply redundant manner across multiple storage technologies. Two copies will exist on an array of six SATA multiplexed helium hard drives which are capable of the high writing speeds required. An additional copy will be on an SSD array, containing sixteen 8 TB drives. Since the data drives will have the highest priority of recovery after the flight is terminated, their enclosures are designed for easy access and unmounting from the payload.

Simultaneously, every event will be sent through a prioritizer running on a Wolf 3170 GPU, which sorts the incoming data with two goals: downlinking enough data for monitoring and diagnostics of payload health and performance, and sending high quality events in case the data drives are not recovered quickly after the flight. Event priority will depend the data rate of telemetry currently available, and the likelihood that it is of scientific interest.

2.4.1 Communication and data transmission

During the initial period of the flight while the payload is within line of sight (LOS) of McMurdo, communication is over 10 Mbit s⁻¹ S-band downlink and Iridium uplink. After this, downlink switches to the Tracking and Data Relay Satellite System (TDRSS), which is 6 kbit s⁻¹. TDRSS also has a high-gain mode, which may be used but needs to undergo evaluation. We are currently looking into the possibility of StarLink, with 40 Mbit s⁻¹ downlink and uplink. It is still to-be-determined if the StarLink antenna is compliant with PUEO's RF noise requirements; however, even if not, we would consider running at a low duty cycle, or during periods when PUEO will be dominated by anthropogenic sources such as McMurdo or South Pole Station.

2.5 Gondola

The PUEO gondola is based on the design from ANITA. It is designed to meet NASA requirements to withstand a load of 8 G vertically, and 4 G horizontally and at 45°. The gondola is made of carbon fiber composite tubes fabricated by RockWest, with aluminum alloy 7075 clevis fastener end caps attached with Loctite Hysol E-120 HP. The aluminum fasteners connect at hub plates, and use titanium pins for quick disassembly during recovery.

PUEO will be suspended beneath a 0.97 Mm³ helium balloon, which has a maximum lifting capacity of 8000 lbs. With current best estimates, the total mass (science plus balloon-specific hardware from NASA) has about 13 % margin.

2.6 Attitude and position determination

PUEO has accuracy requirements of 50 m in position and 0.05° in heading pitch, and roll to ensure that the navigation uncertainty doesn't contribute to the error in direction from interferometry. To achieve this, PUEO will be equipped with an extensive navigation suite, including two inertial navigation systems (INS), a differential GNSS unit, two star trackers, an omnidirectional sun sensor array, and a magnetometer. Since there is not much experience with inertial navigation on a balloon in Antarctica, PUEO will fly two different models. The Advanced Navigation Boreas contains a very precise digital fiber optic gyroscope (DFOG) IMU, and is expected to achieve an accuracy of

$<0.005^\circ$ in pitch and roll, and $<0.01^\circ$ in heading. The CPT7 from Novatel uses a MEMS-based IMU, and is expected to achieve $\sim 0.01^\circ$ in all three angles. The star trackers have not been used on a freely rotation balloon like PUEO, but are expected to achieve similar or better precision.

A Kalman filter running on the flight computer will process the navigation solutions from the entire suite and produce a first estimate of position and attitude in real time. All navigation data will also be stored onboard at a much higher rate, which will allow for post-processing after recovery.

2.7 Power system

PUEO will use a 24-sided omnidirection array of solar panels capable of outputting 1800 W, giving plenty of margin on top of PUEO's designed power requirement of ~ 1246 W. Each panel consists of two vertically stacked 6 cell by 5 cell photovoltaics (PVs). The PV array will begin flight covering the bottom two rings of antennas in order to fit within the launch envelope; immediately after launch a redundant set of hoists will deploy the array. The power system uses a 60 A Morningstar Tristar MPPT charge controller, which has flight heritage from ANITA-III and ANITA-IV, among others. To provide stable power, especially while waiting on the flightline and direct sunlight is not guaranteed, there will be two sets of four in-series 20 A h 12 V lead-acid batteries.

2.8 Calibration

PUEO will use ground-to-payload calibration pulsers located in McMurdo, as well as at remote field camps in Antarctica. There will also be two hand-launched HiCal3 payloads that are modeled after previous HiCal designs, which were part of the ANITA program [15]. They are made of two dual polarized wide band antennas and a high voltage pulser that will emit impulsive signals at a regular cadence for calibration; these will be detected by PUEO both directly and reflected from the ice below.

3. Conclusion

PUEO is on track to fly in December 2025; key design improvements over ANITA, including a phased array trigger, will enable it to make the first detection of UHE neutrinos.

Acknowledgements

We would like to thank NASA for support through grant 80NSSC21M0116.

References

- [1] S. Razzaque and L. Yang, *PeV-EeV neutrinos from GRB blast waves in IceCube and future neutrino telescopes*, *PhRvD* **91** (2015) 043003 [[1411.7491](#)].
- [2] X. Rodrigues, J. Heinze, A. Palladino, A. van Vliet and W. Winter, *Active Galactic Nuclei Jets as the Origin of Ultrahigh-Energy Cosmic Rays and Perspectives for the Detection of Astrophysical Source Neutrinos at EeV Energies*, *PhRvL* **126** (2021) 191101 [[2003.08392](#)].
- [3] K. Greisen, *End to the Cosmic-Ray Spectrum?*, *PhRvL* **16** (1966) 748.

- [4] G.T. Zatsepin and V.A. Kuz'min, *Upper Limit of the Spectrum of Cosmic Rays*, *Soviet Journal of Experimental and Theoretical Physics Letters* **4** (1966) 78.
- [5] P.W. Gorham, P. Allison, S.W. Barwick, J.J. Beatty, D.Z. Besson, W.R. Binns et al., *New Limits on the Ultrahigh Energy Cosmic Neutrino Flux from the ANITA Experiment*, *PhRvL* **103** (2009) 051103 [[0812.2715](#)].
- [6] P.W. Gorham, P. Allison, B.M. Baughman, J.J. Beatty, K. Belov, D.Z. Besson et al., *Observational constraints on the ultrahigh energy cosmic neutrino flux from the second flight of the ANITA experiment*, *PhRvD* **82** (2010) 022004 [[1003.2961](#)].
- [7] P.W. Gorham, P. Allison, O. Banerjee, L. Batten, J.J. Beatty, K. Bechtol et al., *Constraints on the diffuse high-energy neutrino flux from the third flight of ANITA*, *PhRvD* **98** (2018) 022001 [[1803.02719](#)].
- [8] P.W. Gorham, P. Allison, O. Banerjee, L. Batten, J.J. Beatty, K. Belov et al., *Constraints on the ultrahigh-energy cosmic neutrino flux from the fourth flight of ANITA*, *PhRvD* **99** (2019) 122001 [[1902.04005](#)].
- [9] G.A. Askar'yan, *Coherent Radio Emission from Cosmic Showers in Air and in Dense Media*, *Soviet Journal of Experimental and Theoretical Physics* **21** (1965) 658.
- [10] P.W. Gorham, S.W. Barwick, J.J. Beatty, D.Z. Besson, W.R. Binns, C. Chen et al., *Observations of the Askaryan Effect in Ice*, *PhRvL* **99** (2007) 171101 [[hep-ex/0611008](#)].
- [11] Q. Abarr, P. Allison, J. Ammerman Yebra, J. Alvarez-Muñiz, J.J. Beatty, D.Z. Besson et al., *The Payload for Ultrahigh Energy Observations (PUEO): a white paper*, *Journal of Instrumentation* **16** (2021) P08035 [[2010.02892](#)].
- [12] C. Deaconu, Q. Abarr, P. Allison, J. Alvarez-Muñiz, J. Ammerman Yebra, T. Anderson et al., *Searching for Askaryan Emission from Neutrinos with the Payload for Ultrahigh Energy Observations (PUEO)*, in *Proceedings of 38th International Cosmic Ray Conference — PoS(ICRC2023)*, vol. 444, p. 1031, 2023, [DOI](#).
- [13] K. Hughes, Q. Abarr, P. Allison, J. Alvarez-Muñiz, J.A. Yebra, T. Anderson et al., *Identifying and Characterizing Air Shower Events with the Payload for Ultrahigh Energy Observations (PUEO)*, in *Proceedings of 38th International Cosmic Ray Conference — PoS(ICRC2023)*, vol. 444, p. 1027, 2023, [DOI](#).
- [14] P. Allison, S. Archambault, R. Bard, J.J. Beatty, M. Beheler-Amass, D.Z. Besson et al., *Design and performance of an interferometric trigger array for radio detection of high-energy neutrinos*, *Nuclear Instruments and Methods in Physics Research A* **930** (2019) 112 [[1809.04573](#)].
- [15] S. Prohira, A. Novikov, D.Z. Besson, K. Ratzlaff, J. Stockham, M. Stockham et al., *HiCal 2: An instrument designed for calibration of the ANITA experiment and for Antarctic surface reflectivity measurements*, *Nuclear Instruments and Methods in Physics Research A* **918** (2019) 60 [[1710.11175](#)].

Full Authors List: PUEO Collaboration

Q. Abarr¹, P. Allison², J. Alvarez-Muñiz³, J. Ammerman Yebra³, T. Anderson⁴, A. Basharina-Freshville⁵, J. J. Beatty², D. Z. Besson⁶, R. Bose⁷, D. Braun⁷, P. Chen⁸, Y. Chen⁸, J. M. Clem¹, T. Coakley², A. Connolly², L. Cremonesi⁹, A. Cummings⁴, C. Deaconu¹⁰, J. Flaherty², P. W. Gorham¹¹, C. Hornhuber⁶, J. Hoffman⁷, K. Hughes⁴, A. Hynous¹², M. Jackson², A. Jung¹¹, Y. Ku⁴, C.-Y. Kuo⁸, G. Leone¹⁰, C. Lin¹, P. Linton², T. C. Liu¹³, W. Luszczak², S. Mackey¹⁰, Z. Martin¹⁰, K. McBride², C. Miki¹¹, M. Mishra¹¹, J. Nam⁸, R. J. Nichol⁵, A. Novikov¹, A. Nozdrina⁶, E. Oberla¹⁰, S. Prohira⁶, R. Prechelt¹¹, H. Pumphrey⁵, B. F. Rauch⁷, R. Scrandis¹⁰, D. Seckel¹, M. F. H. Seikh⁶, J. Shiao⁸, G. Simburger⁷, G. S. Varner¹¹, A. G. Viereg¹⁰, S.-H. Wang⁸, C. Welling¹⁰, S. A. Wissel⁴, C. Xie⁵, R. Young⁶, E. Zas³, A. Zeolla⁴

¹University of Delaware, ²Ohio State University, ³Universidade de Santiago de Compostela, ⁴Pennsylvania State University, ⁵University College London, ⁶University of Kansas, ⁷Washington University in St. Louis, ⁸National Taiwan University, ⁹Queen Mary University of London, ¹⁰University of Chicago, ¹¹University of Hawaii, ¹²NASA Wallops Flight Facility, ¹³National Pingtung University